FINAL REPORT

PREDICTING THE SPATIAL VARIABILITY OF SITE RESPONSE

Award: 05HQGR0059

Element II: Evaluate Urban Hazard and Risk

Ralph J. Archuleta

Institute for Crustal Studies
University of California, Santa Barbara

Research supported by the U. S. Geological Survey (USGS), Department of Interior, under USGS award number 05HQGR0059. The views and conclusions contained in this document are those of the authors and should not be interpreted as necessarily representing the official policies, either expressed or implied, of the U. S. Government.

Award: 05HQGR0059

PREDICTING THE SPATIAL VARIABILITY OF SITE RESPONSE

Ralph J. Archuleta
Institute for Crustal Studies
University of California, Santa Barbara 93106
Phone: 805-893-8441
FAX: 805-893-8649
Email: ralph@crustal.ucsb.edu

TECHNICAL ABSTRACT

Estimation of the spatial variation of frequency-dependent site amplification factors has been investigated based on the data of the very dense Yokohama array network. First, we took two groups of events based on its focal depth and calculated ground motion parameters, such as PGA, PGV, and Duration. The statistical analysis of the parameters showed that the spatial variation of each parameter seems to be correlated with the distribution of average shear wave velocities for upper 30m. Next, using a nonlinear algorithm, we inverted the data from the borehole accelerometers to determine site response, source parameters, and path attenuation parameters. Having determined the critical parameters of the path and the source we directly computed the frequency dependent site response for all 150 surface stations as follows: for 17 deep events and four shallow events we computed the predicted spectrum based on our knowledge of the path and source parameters gained from inversion of the borehole records. For each site and for each event we calculated the misfit between the observed and predicted amplitude spectrum and then averaged over all the events to determine a site response for each of the 150 surface stations. For frequencies less than 3.0 Hz the average site response correlates with average shear wave velocities for upper 30m. If the two sites have similar AVS30 values, we found that for frequencies up to 1.0 Hz, the unknown site response has a 95% probability of differing by less than a factor of 2 from a known site response. By constructing cumulative probability curves, we show that there is a 90% probability that site response coefficients will differ by less than a factor of 3 for frequencies up to 10.0 Hz. In the case where the two sites have the least similar AVS30, we found that for all six frequencies, 80% of the predictions for an unknown site response would be within a factor of 3 of a known site response for separation distances up to 5 km. Thus for all 2262 station pairs we would infer that the site response can be predicted within a factor of 3 with 80% probability for all frequencies up to 10 Hz.

The density of the Yokohama accelerometer network coupled with the completeness of the site characterization has allowed us to quantify site response as a function of station separation and frequency. This analysis provides, for the first time, a detailed quantitative look at how the amplitude of the site response varies with regard to distance, frequency and local shear wave velocity. It may provide a better understanding of the predictability of ground motion from future earthquakes.

Introduction

Quantifying the spatial variation of site response from event-to-event and site-to-site requires a dense set of stations as well as multiple events. The Yokohama high-density strong ground motion network constructed by the city of Yokohama has 150 stations within very small area. The analysis of this very unique array data made it possible to estimate the spatial variation of site response within a limited area, but the lessons learned from analysis of the data can be applicable to other general cases. The array has 150 surface stations with 3-component accelerometers and nine borehole sites with instruments at depths between 16 and 69 m. The surface stations cover an area 434 km^2 that is approximately 25 km x 20 km with spacing on the order of 2 km with many sites much closer together. We analyzed data from 29 earthquakes (Table 1) ranging in magnitude M_W 4.0–7.3, depths in the range 3–430 km and azimuthal coverage of nearly 270˚ (Figure 1). In this study, we first have analyzed ground motion parameters statistically and compared to the geotechnical parameters related to the structure at each site. Next, to quantify the spatial variation of site response, we computed site response for each of the 150 stations. Using the nine borehole stations we nonlinearly invert for the source and path parameters for each event. The site response for each surface station is easily computed as the difference between the average computed spectrum and the average observed spectrum.

Yokohama Seismic Array

The city of Yokohama, located southwest of Tokyo, has the densest array of strong motion accelerometers anywhere in the world [1], [2], [3]. The array has 150 surface stations with 3-component accelerometers and nine borehole sites with instruments at depths between 16 and 69 m. The surface stations cover an area 434 km^2 that is approximately 25 km x 20 km with spacing on the order of 2 km with many sites much closer together. We analyzed data from 29 earthquakes (Table 1) ranging in magnitude M_W 4.0–7.3, depths in the range 3–430 km and azimuthal coverage of nearly 270˚ (Figure 1). The Yokohama seismic array was designed to provide real-time assessment of damage and to provide strong-motion data for improving construction that would make Yokohama more resistant to earthquake damage [1]. The array, completed in May 1997, consists of 150 three-component surface stations supplemented by 9 borehole stations (Figure 2). Each station has descriptions of the local P and S wave velocities as well as the lithology for the near surface (10–70 m). The 9 borehole stations range in depth from 20 to 70 m, approximately; the surface station spacing is approximately 2 km with many stations at smaller separation spacing.

By correlating measured shear wave velocities at the 150 accelerometer sites with the local geology the four basic lithological units are given estimated velocities for the near surface: reclaimed land, 120–190 m/s; Holocene sediments, 140-400 m/s; Pleistocene sediments, 130-500 m/s and late Tertiary sediments, > 700 m/s [3]. However, when averaged over the upper 30 m, most of the area has an average S–wave velocity near 300 m/s. The basin structure underlying Yokohama is part of the greater Kanto basin. The contours of the P wave velocity indicate that Yokohama city sits above the western boundary of the deepest part of the basin, approximately 3.5–4.0 km [5], [6]. We assumed the base has a Poisson ratio of 0.25, an S-wave velocity of 3.1 km/s with a corresponding P-wave velocity 5.37 km/s

Table 1: Location and Magnitudes of Earthquakes Recorded on Yokohama Array

	Event	Lat.	Long.	Depth (km)	Mw	Moment (Nm)	No. Surface Stns.	No. Boreholes
1	1/14/98	35.59	140.24	76	4.9	2.28E+16	149	0
2	1/16/98	35.21	140.25	57	4.5	5.36E+15	148	0
3	4/26/98	34.96	139.17	5	4.7	3.46E+16	137	0
4	5/3/98	34.95	139.18	3	5.5	2.34E+17	149	9
5	5/16/98	34.97	139.94	74	4.7	1.49E+16	150	9
6	6/14/98	35.44	140.76	51	5.7	3.58E+17	146	0
7	8/29/98	35.6	140.05	67	5.3	9.80E+16	149	9
8	11/8/98	35.61	140.05	78	4.7	1.36E+16	150	9
9	11/28/98	35.63	140.10	67	4.3	3.29E+15	144	9
10	12/3/98	35.61	140.04	67	4.4	3.87E+15	142	9
11	3/26/99	36.45	140.62	58	5.1	4.55E+16	98	0
12	4/25/99(18:00)	35.52	140.30	92	4.4	4.49E+15	144	7
13	4/25/99(21:00)	35.46	140.63	58	5.2	6.24E+16	104	5
14	5/7/99	35.22	138.35	20	4.8	1.56E+16	75	0
15	5/22/99	35.45	139.19	23	4.1	1.61E+15	148	9
16	7/15/99	35.92	140.46	56	5.1	5.33E+16	126	6
17	8/9/99	35.83	139.96	116	4.6	8.17E+15	106	9
18	8/11/99	35.4	139.83	62	4.0	9.93E+14	133	6
19	9/13/99	35.57	140.20	77	5.3	1.08E+17	150	9
20	2/11/00	35.5	139.05	18	4.2	2.29E+15	149	9
21	4/10/00	35.19	140.07	55	4.7	1.26E+16	142	9
22	6/3/00	35.68	140.72	48	6.1	1.72E+18	147	9
23	8/6/00	28.86	140.07	430	7.3	1.20E+20	142	9
24	8/27/00	35.76	140.14	77	4.6	9.31E+15	126	8
25	9/29/00	35.5	139.70	90	4.8	1.83E+16	148	9
26	9/18/01	35.4	139.80	51	4.5	5.59E+15	144	9
27	12/8/01	35.5	139.10	30	4.5	6.13E+15	146	9
28	11/3/02	38.9	142.10	50	6.4	3.87E+18	97	6
29	3/13/03	36.1	139.90	50	4.9	2.34E+16	133	8

These parameters were determined by National Institute for Earth Science and Disaster Prevention (NIED), Tsukuba, Japan except for the seismic moment of Event 23, which was determined by Kikuchi and Yamanaka [4].

Statistical Analysis of Ground Motion Parameters

The site response has for the nine borehole stations had been determined previously from six earthquakes [2]. Seven of nine borehole site responses were fairly well predicted by the velocity logs. Seven earthquakes recorded on all the stations have been used to determine site response, in particular to determine the fundamental period and the amplitude of the fundamental period at each site [7]. They found that the theoretical site response, based on the local logs of *in situ* P and S-wave velocities, predicted almost 95% of the peak amplitudes and periods within a factor of two. For all these 29 events we have computed the same ground motion parameters that

are given in the headings of Table 2. To illustrate some of our results we take three groups of earthquakes, we used the data from 21 events with borehole records. Since the hypocenters for events 23 and 28 are too far from this array we did not use the data from these events. To illustrate some of our results, we take three groups of earthquakes: 4 shallow events, 7 deep events (4.0 ≦M≦ 4.6), and 10 deep events (4.7 ≦M≦ 5.3) based on the focal depth and magnitude (Table 1) With each group we have tried to examine the relationship of the ground motion parameters—Cumulative Absolute Velocity (CAV), Spectral Intensity (SI) Arias Intensity (AI), Peak Ground Acceleration (PGA), Peak Ground Velocity (PGV) and Duration (Dur)—with the average shear wave velocity for upper 30 m (ASV30). We only use 2 horizontal components and took vector summation of them, while taking average of them only for duration. We divided the ASV30 into 7 bins: 0-200 m/s (12 stations), 200-250 m/s (11), 250-300 m/s (19), 300-350 m/s (35), 350-400 m/s (35) and 400-700 m/s (17). The value of ASV30 is based on logs for depths for each station. We derived a mean value of the ground motion parameter and the standard deviation of the mean using the number of stations in each velocity bin. The results are shown in Figures 2. The most obvious result of this work is that within a group of shallow events and larger deep events, there is a clear trend of these three parameters with the ASV30 except for AI and PGA. However, the parameters seem to be independent of the ASV30 except for SI and Dur for small deep events. Specially, within these parameters, SI and Dur show very good correlation with ASV30. (Correlation coefficients for SI are -0.82 for shallow, -0.62 for smaller deep, and -0.93 for larger deep events, and for Dur are -0.86 for shallow, -0.76 for smaller deep, and -0.85 for larger deep events). On the other hand, PGA, AI showed little correlation for all three groups.

To examine if there might be a spatial correlation with ASV30 that would not show up in these figures we have contoured the averaged variables on maps of ASV30 for these events in Figures 3a, b. Although it is too preliminary to draw any conclusions, there are certain areas of the city where SI, AI, CAV seem to peak independent of event group. And these are the same areas that show the low velocity area at the northern part of the city. Further calculations are needed to confirm if these conclusions about the spatial correlation can be accounted for by a single variable such as shallow shear wave velocity.

Site Response

In a previous section, some ground motion parameters are estimated. However, those parameters include not only site response, but source and path effects. To estimate the spatial variation of site response more quantitatively, it is necessary to separate the site response from the observed records. The observed ground motion generally can be expressed a convolution of the source, path and site. To estimate the spatial variation of site response, it is necessary to separate those three quantities analytically. Because of the unique data set we have to devise a method for separating these quantities. In the frequency domain, we can write the convolution as a multiplication: $A(f) = S(f)P(f)Site(f)$ where f is frequency, $A(f)$ is the spectrum of the recorded ground motion, $P(f)$ is the path effect, which is modeled as frequency dependent attenuation $Q(f) = Q_o f^{\gamma}$ in this study, and $Site(f)$ is the site response. However, the source has a nonlinear dependence on the corner frequency assuming an f^2 model: $S(f) = CM_o(2\pi f)^2 f_c^2 \big/ \left(f^4 + f_c^4\right)^{0.5}$ where C is a constant that depends on distance from source to site, radiation parameter of the source and material parameters; M_o is seismic moment that is related to the size of the earthquake and f_c is the corner frequency that controls the high

frequency shape of the spectrum [8], [9]. The path effect also has a nonlinear dependence on frequency if we assume that the attenuation parameter (damping) has a power law dependence on frequency $Q(f) = Q_o f^{\gamma}$. Of the the corner frequency that controls the high frequency shape of the spectrum [24], [25]. The path effect also has a nonlinear dependence on frequency if we assume that the attenuation parameter damping has a power law dependence on frequency $Q(f) = Q_o f^{\gamma}$. Of the 21 events used by statistical analysis used in the previous section, we picked 13 events (9 deep events and 4 shallow events) that are best recorded at borehole stations to be used as reference events. The record section used for this inversion starts 1.0 s before the direct S-wave arrival and has a length 10.0 s. We use the data to estimate: the source parameters (M_o, f_c), the attenuation parameters for the path (Q_o, γ) and the frequency dependent site effect $Site(f)$. The quality factor Q (equivalent to 1/(2xdamping) in engineering terms) is assumed to be constant for frequencies less than 1.0 Hz while having a power law relation for frequencies greater than 1.0 Hz. Because of the spectrum is not linearly related to the corner frequency and the attenuation parameter g we need to solve a nonlinear problem. We use a Heat Bath algorithm [26] to invert for the parameters: M_o , f_c ,Q_o, g and the frequency dependent site response. The overall approach is iterative as explained later. We used only the data from nine deep events recorded on the borehole accelerometers. Initially we assume that the borehole response is a constant. Under this assumption we invert the data for all nine events to determine M_o, f_c, Q_o, g. The difference between the observed and predicted spectrum is taken as our first estimate of the site response. Our next step is to use this estimate of the site response and invert for M_o using only the spectrum f ≤ 1.0 Hz. With this estimate of the seismic moment and the site response we again invert all of the data to find f_c, Q_o, g. This produces the second estimate of the site response as

Table 2: Source Parameters Derived by Inversion

Event	Date	Mo [Nm]	M_W	f_c[Hz]	Stress Drop (bars)
4*	5/3/98	2.08E+16	4.8	1.9	216
5	5/16/98	2.16E+16	4.9	2.4	268
7	8/29/98	1.22E+17	5.4	1.2	195
8	11/8/98	2.56E+16	4.9	2	195
9	11/28/98	5.04E+15	4.4	3	131
10	12/3/98	7.23E+15	4.5	2.5	101
12	1999/4/25_1	6.95E+15	4.5	3.8	345
13	1999/4/25_2	3.76E+16	5.0	1.4	86
15*	5/22/99	3.46E+15	4.3	2.4	69
16	7/15/99	3.43E+16	5.0	1.1	45
17	8/9/99	9.04E+15	4.6	4.7	841
18	8/11/99	2.75E+15	4.3	2.8	55
19	9/13/99	8.54E+16	5.3	1.5	272
20*	2/11/00	6.63E+15	4.5	2.1	93
21	4/10/00	1.28E+16	4.7	1.5	42
22	6/3/00	2.82E+17	5.6	0.6	68
24	8/27/00	1.39E+16	4.7	1.9	90
25	9/29/00	3.38E+16	5.0	1.5	95
26	9/18/01	1.41E+16	4.7	1.4	32
27*	12/8/01	1.05E+16	4.6	1.7	81
29	3/13/03	3.37E+16	5.0	1.1	38

*Indicates a shallow event (hypocentral depth ≤ 30 km)

the difference between the predicted (based on the current values of M_o, f_c, Q_o, g) spectrum and the observed spectrum. We iterate this procedure until the residuals between observed and predicted spectra are negligible. Thus we derive a frequency dependent site response for each of the borehole stations as well as solving for the path parameters Q_o, g. Now that we have stable values of the site response and path effect, we invert the data from each of the 17 deep events with borehole data to find M_o, f_c (Table 2). The same procedure is applied to four shallow events, but there are differences in the material properties of the medium between the deep and shallow events. From this analysis we find a frequency dependent Q for deep events $Q(f) = 284 f^{0.06}$ which is almost independent of frequency. However for the shallow events we find stronger frequency dependence, $Q(f) = 74 f^{0.28}$. The quality of the inversion procedure is illustrated in Figure 7 where we plotted the predicted spectrum for nine borehole stations. The borehole response at each station is also shown. The agreement between the observed and predicted spectrum from 0.5-30 Hz is excellent (Figure 7).

Knowing M_o, f_c, Q_o, g we can predict the spectra for all 150 surface sites for each event. The difference between the predicted and observed spectrum is the frequency dependent site effect. Thus we could construct the basic data set that allows us to quantify the spatial variation of the site response. With 17 deep events and 4 shallow events, we can examine the variability of the ground response from event to event as well as compare deep and shallow excitation. With 150 stations we looked at the variation from site-to-site; with 21 events (17 deep events and 4 shallow events), we can examine event-to event variations.

In Figure 4, we contoured the average site amplification (average of 17 deep events) for three frequency ranges: 0.5–1.0, 1.0–3.0 and 3-10.0 Hz. As might be expected, the low frequency (0.5–1.0 Hz) contours are fairly uniform except around stations with a large site response.

Spatial Variation of Site Response

As seen in Figure 4, site response within the Yokohama array shows significant variation even for stations separated by less than 1.0 km. To examine how this site response might vary as a function of both frequency and distance we introduce a site correlation factor. Borrowing from the normal definition of correlation we define a site response correlation SRC_{ij} as

$$SRC_{ij} = \frac{2Site_i(f)Site_j(f)}{\left(Site_i(f)\right)^2 + \left(Site_j(f)\right)^2}$$

where $Site_i(f)$ is site amplification for the ith station and $Site_j(f)$ is site amplification for the jth station. The SRC_{ij} is normalized so that if the two site responses are identical, it will take on a maximum value of 1.0; the minimum value is 0.

To see what the predictive capabilities might be, we contour $SRC(f)^+$ as a function of frequency and separation distance for 466 the station pairs with the most similar site condition (Figure 10). We have done the same for the 466 pairs with the least similar site condition, but the plot is not shown although we have analyzed these data as described below. As seen in the histogram for the number of stations versus station separation (Figure 5), there is limited data for station pairs with a separation distance less than 600 m. Consequently we have examined only data for separation distances of 300 m and greater. There is a gap in the data between 500 and 600 m; contours in this range are an artifact of the contouring program. The number of station pairs with separation distance more than 600 m is rather uniform. The value of $SRC(f)^+$

determined by pairs of stations tends to increase with increasing frequency; for example, for the frequencies less than 1.0 Hz, this value is mostly less than 1.5.

To understand better how the site response coefficient varies with distance we consider six frequencies. For each frequency we plot the cumulative probability versus the site response coefficient (Figure 6). We do this for both the most similar and least similar site conditions. For each frequency, the upper panel shows $SRC(f)^+$ as a function of distance; the corresponding lower panel shows the cumulative probability as a function of $SRC(f)^+$. We mark the cumulative probability where the $SRC(f)^+$ value is a factor of two (Figure 6).

We have tried to model each cumulative probability function as a smooth parametric function assuming the following form:

$Cum\left(SRC(f)^+, f\right) = 1 - \left[\exp\left\{-(SRC(f)^+ - 1)/a\right\}\right]$. For each of the frequencies plotted in Figure 6, we solved for the parameter *a* by non-linear regression. The values of *a* and residuals (=∑ (data-*Cum*)² / (number of data)) are given in Table 3 for both the most similar and least similar AVS30 ratio.

Table 3: Regression Parameters

	Most Similar AVS30		Least Similar AVS30	
Frequency [Hz]	*a*	Residuals	*a*	Residuals
0.5	0.17	7.5E-04	0.37	3.7E-04
0.75	0.26	5.4E-04	0.67	2.3E-03
1	0.28	9.1E-04	0.84	3.1E-03
2	0.61	6.9E-04	0.86	7.1E-04
5	0.65	3.5E-04	0.73	4.9E-04
10	0.79	1.0E-03	0.99	4.4E-04

Summary

Because of the density of sites, we developed two functions—a site response correlation and a site response coefficient—that allowed us to quantify different site responses as well as to predict site responses in both the frequency and spatial domains. We use the site response coefficient to predict an unknown site response for distances up to 5 km from a site with a known site response. If the two sites have similar AVS30 values, we found that for frequencies up to 1.0 Hz, the unknown site response has a 95% probability of differing by less than a factor of 2 from a known site response. By constructing cumulative probability curves (Figure 6), we show that there is a 90% probability that site response coefficients will differ by less than a factor of 3 for frequencies up to 10.0 Hz. In the case where the two sites have the least similar AVS30, we found that for all six frequencies, 80% of the predictions for an unknown site response would be within a factor of 3 of a known site response for separation distances up to 5 km. Thus for all 2262 station pairs we would infer that the site response can be predicted within a factor of 3 with 80% probability for all frequencies up to 10 Hz.

The variation of site response comes from event-to-event variation and site-to-site variation. The site-to-site variation has been conventionally estimated by using coherence between two sites (e.g., [10], [11], [12]); such studies are based on the difference in phase of two signals at two sites. These studies show that the coherency, for frequencies of 1.0 Hz and greater,

is less than 0.5 if two sites are separated by more than 1.0 km. In our study we have concentrated on the amplitude of the site response and how it varies from site to site. If one averages over all distances, the average site response coefficients vary by less than a factor of two between 0.5 and 10 Hz with a standard deviation of about 1.5 and 2.0 for sites with similar AVS30 and dissimilar AVS30, respectively.

The density of the Yokohama accelerometer network coupled with the completeness of the site characterization has allowed us to quantify site response as a function of station separation and frequency. This analysis provides, for the first time, a detailed quantitative look at how the amplitude of the site response varies with regard to distance, frequency and local shear wave velocity. It may provide a better understanding of the predictability of ground motion from future earthquakes.

REFERENCES

1. Torii M, Abe S, Suzuki M, Shinbo Y, Aoki T, Shintaro S, Saito M, and Midorikawa S, "Investigation for earthquake disaster mitigation using the dense strong motion network in Yokohama." Irikura, K., Kudo, K, Okada, H., Sasatani, T., Editors. Effects of Surface Geology on Seismic Motion, Vol.1, Rotterdam: AA Balkema, 1998:341-350.
2. Tsuboi S, Saito M, and Ishihara Y. "Verification of horizontal-to-vertical spectral ratio technique for estimation of the site response using borehole seismographs." Bull. Seism. Soc. Am. 91, 2001: 499-510.
3. Tsuda, K. "Inversion of ground motion spectra for site response at 150 stations of a dense accelerograph array." Master's thesis, University of Tokyo, 2001.
4. Kikuchi M, and Yamanaka Y. "EIC seismological notes." http://wwweic.eri.u-tokyo.ac.jp/EIC/EIC_News/
5. Koketsu K, and Higashi S. "Three-dimensional topography of the sediment/basement interface in the Tokyo metropolitan area, central Japan." Bull. Seism. Soc. Am. 82**,** 1992: 2328-2350.
6. Koketsu K, and Kikuchi M. "Propagation of seismic ground motion in the Kanto basin, Japan." Science. 288, 2000: 1237-1239.
7. Kramer SL. "Geotechnical Earthquake Engineering, Prentice-Hall, Upper Saddle River NJ, 1996..
8. Brune JN. "Tectonic stress and the spectra of seismic shear waves from earthquakes." J. Geophys. Res., 75, 1970: 4997-5009.
9. Boatwright J. "Detailed spectral analysis of two small New York State earthquakes." Bull. Seism. Soc. Am, 68, 1978: 1117-1131.
10. Harichandran, R. S. (1999). Spatial variation of earthquake ground motion, Michigan State University, http://www.msu.edu/~harichan.
11. Abrahamson NA, Schneider JF, and Stepp JC. "Empirical spatial coherency functions for application to soil-structure interaction analyses." Earthquake Spectra, 7, 1991: 1-27.
12. Zerva A, and Zhang O. "Estimation of signal characteristics in seismic ground motions." Probabilistic Eng. Mech, 11, 1996: 229-242.

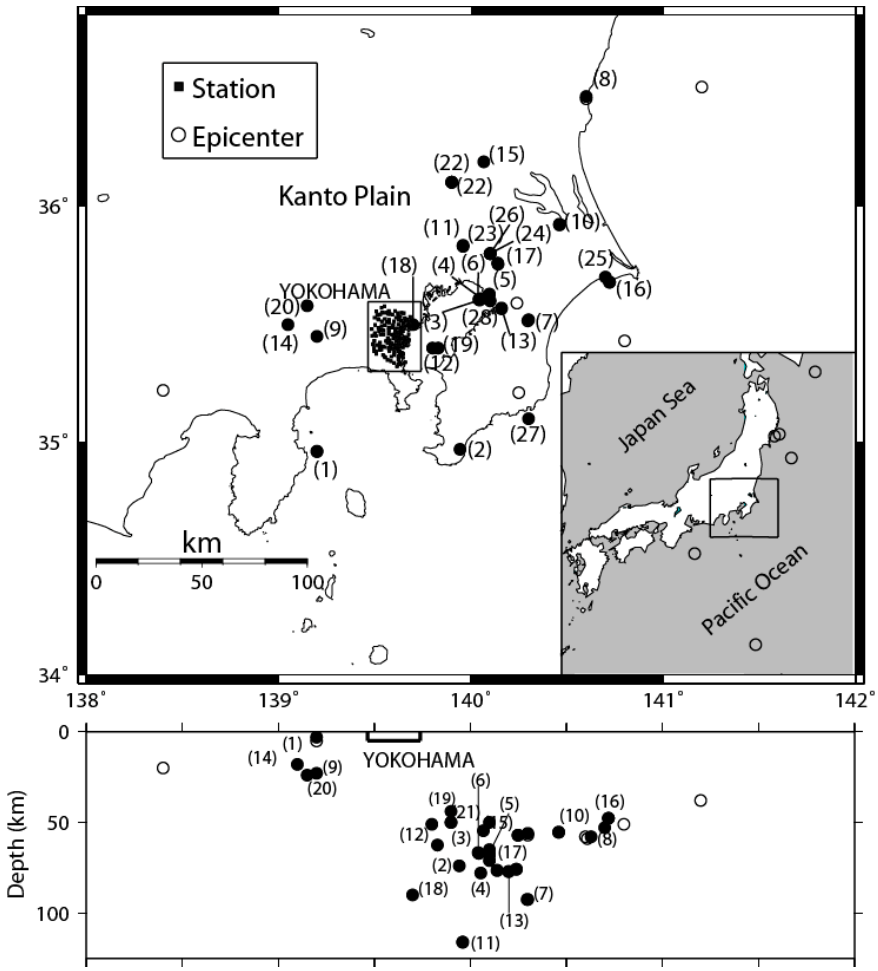

Figure 1: Distribution of epicenters and hypocenters for 29 earthquakes recorded on the 150 element array in Yokohama. Inset shows Japan and the location of the area of detail centered on Yokohama, a city with 3.4 million inhabitants.

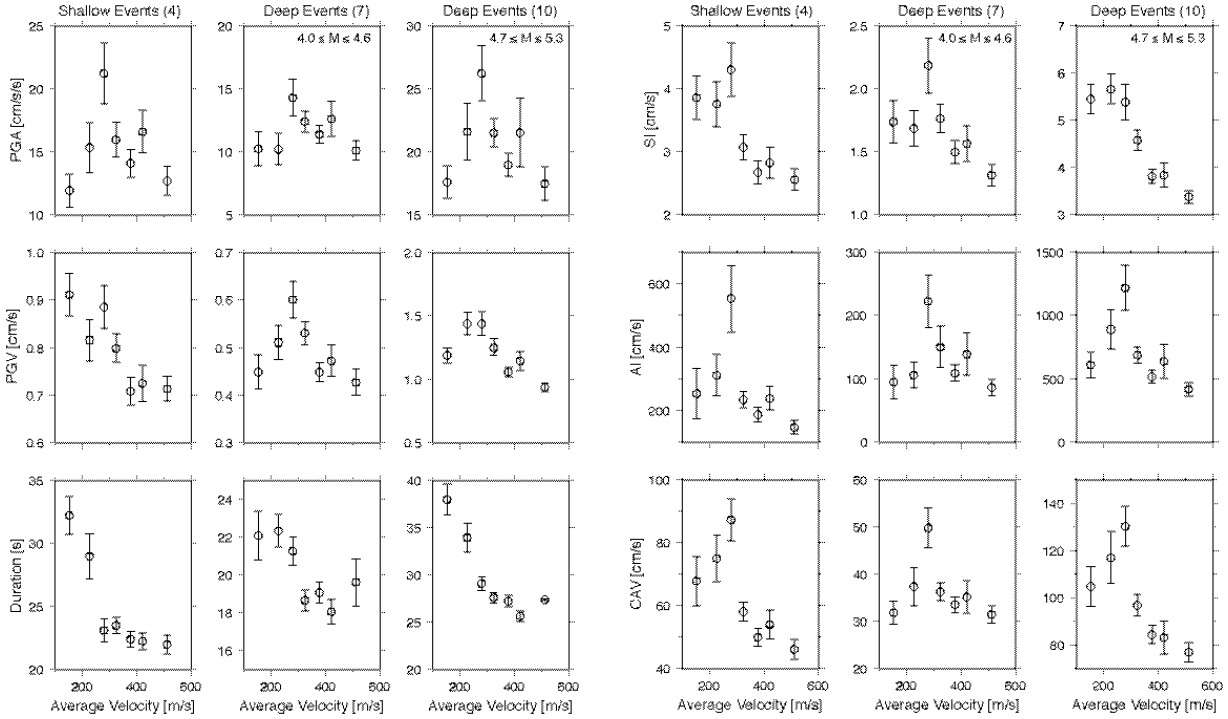

Figure 2: Calculated spectral parameters: PGA, PGV, and Duration (DUR) for the 21 events used for inversion. Each station has been binned into 7 groups based on the AVS30. 'Deep' events are divided into 2 groups with 7 events with **M** 4.0 - 4.6 and 10 events with **M** 4.7 – 5.3. Calculated spectral parameters: SI, AI and CAV for the same events.

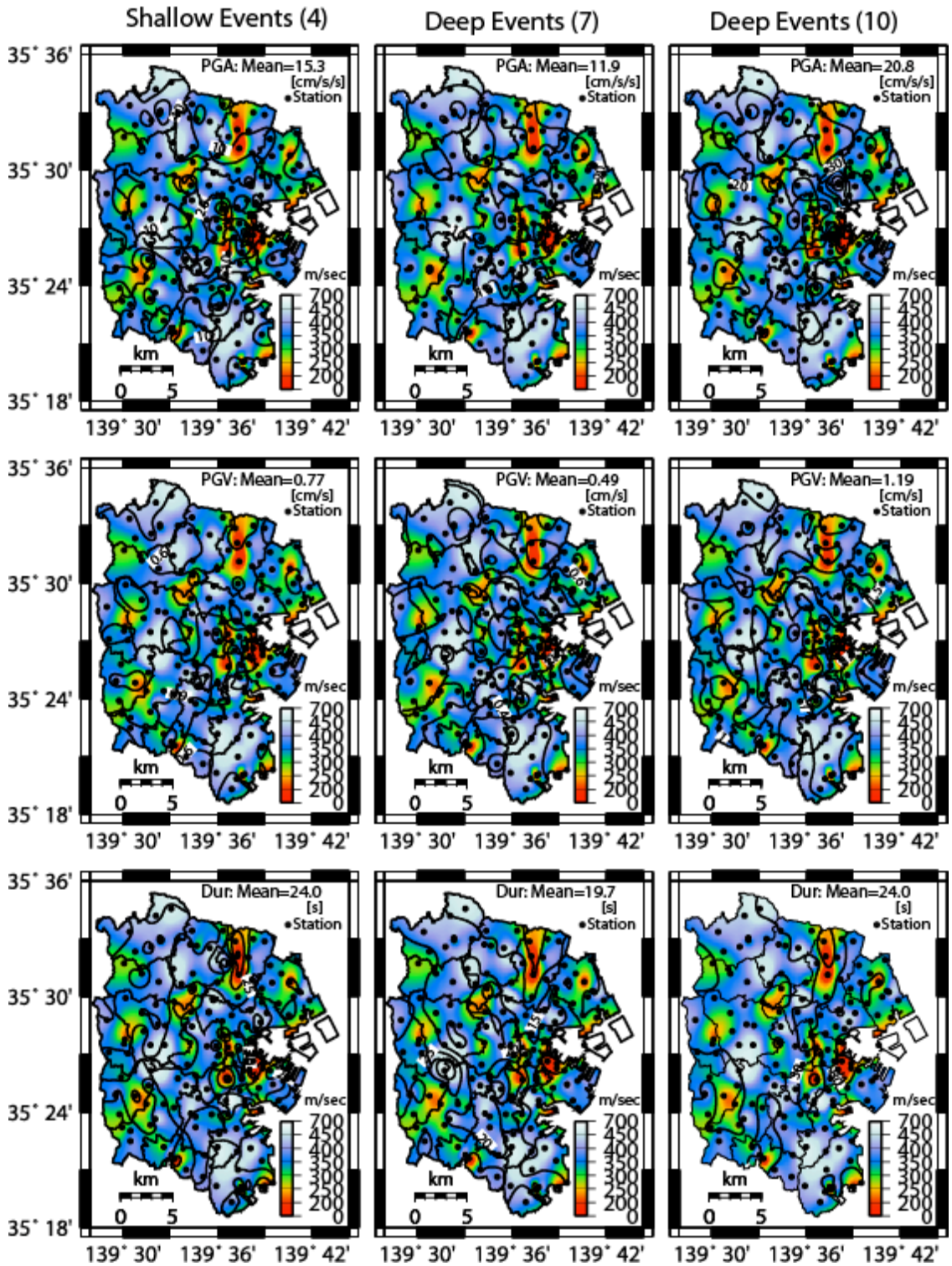

Figure 3a: Contours of PGA, PGV and DUR for the 21 events used for inversion. Each station has been binned into 7 groups based on the AVS30. 'Deep' events are divided into 2 groups with seven events with **M** 4.0 - 4.6 and 10 events with **M** 4.7 – 5.3.

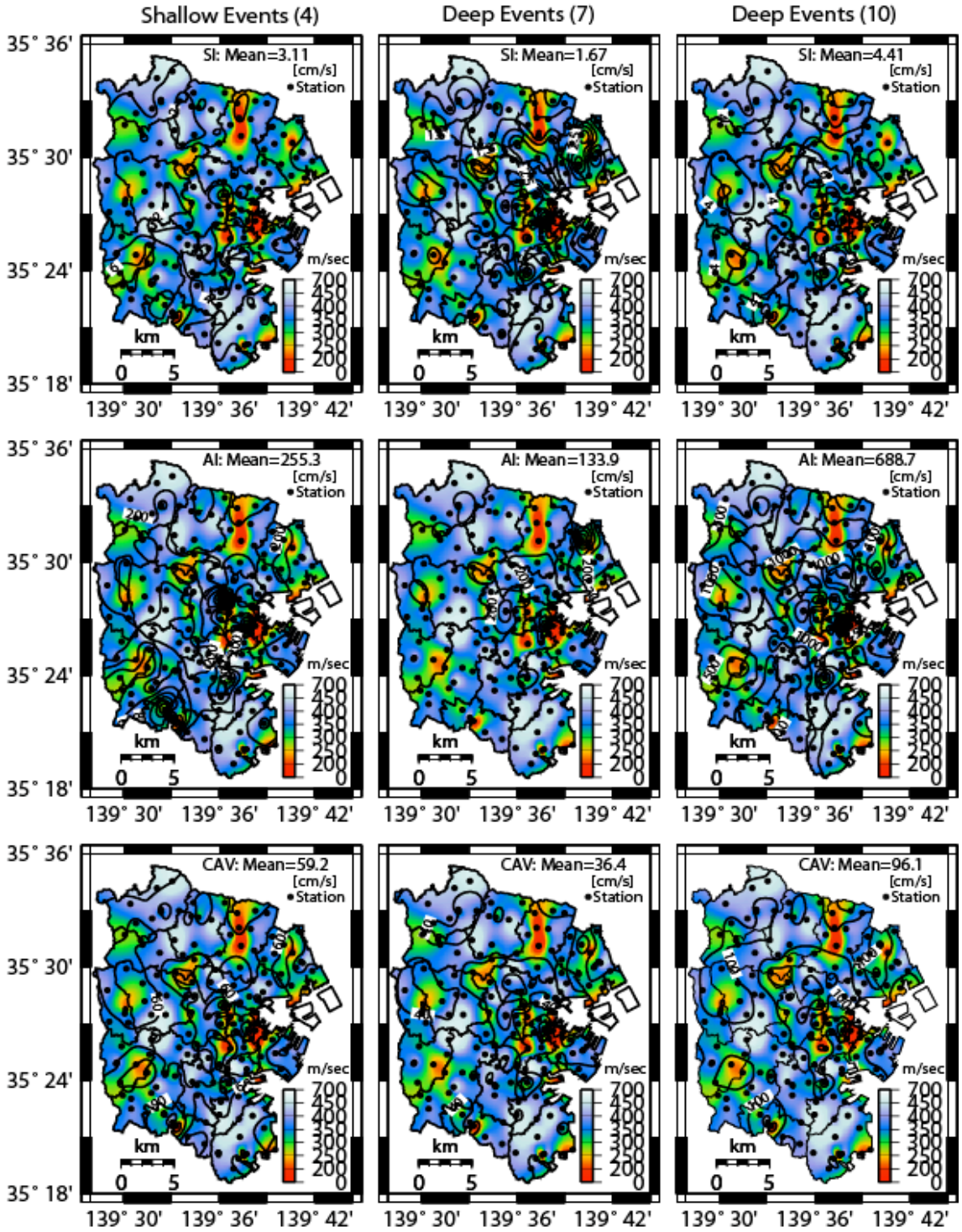

Figure 3b: Contours of SI, AI and CAV for the 21 events used for inversion. Each station has been binned into 7 groups based on the AVS30. 'Deep' events are divided into 2 groups with seven events with **M** 4.0 - 4.6 and 10 events with **M** 4.7 – 5.3.

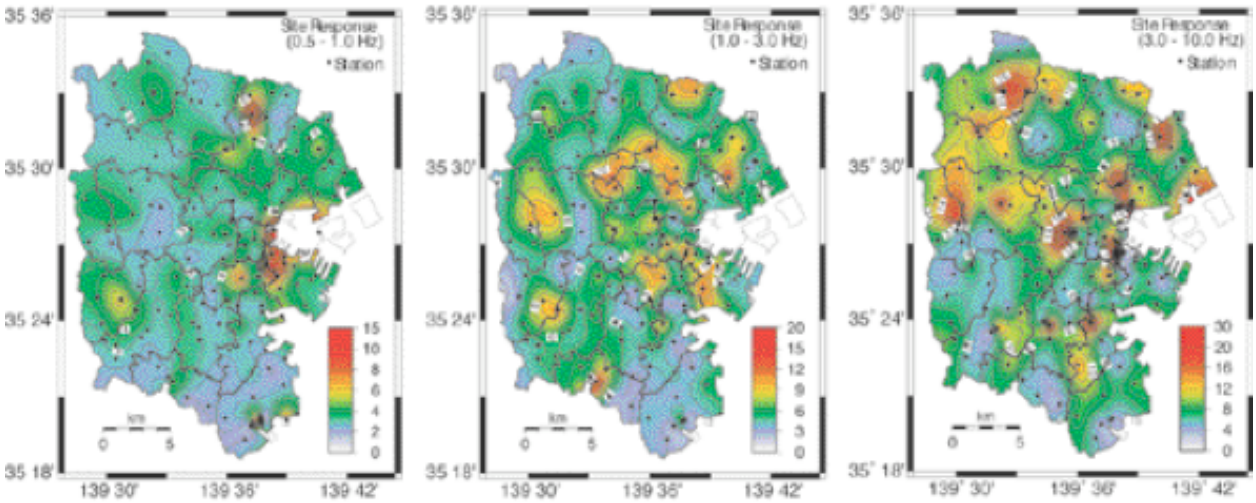

Figure 4: The mean site amplification is computed from 17 deep earthquakes. We computed average value of the site amplification in the frequency bands 0.5–1.0 Hz, 1.0–3.0 Hz and 3.0-10.0 Hz. The average amplification in these three frequency bands is contoured over the area of Yokohama. The frequency band 3.0–10.0 Hz shows broader scale amplification than the lower band even though the lower band has areas of maximum amplification.

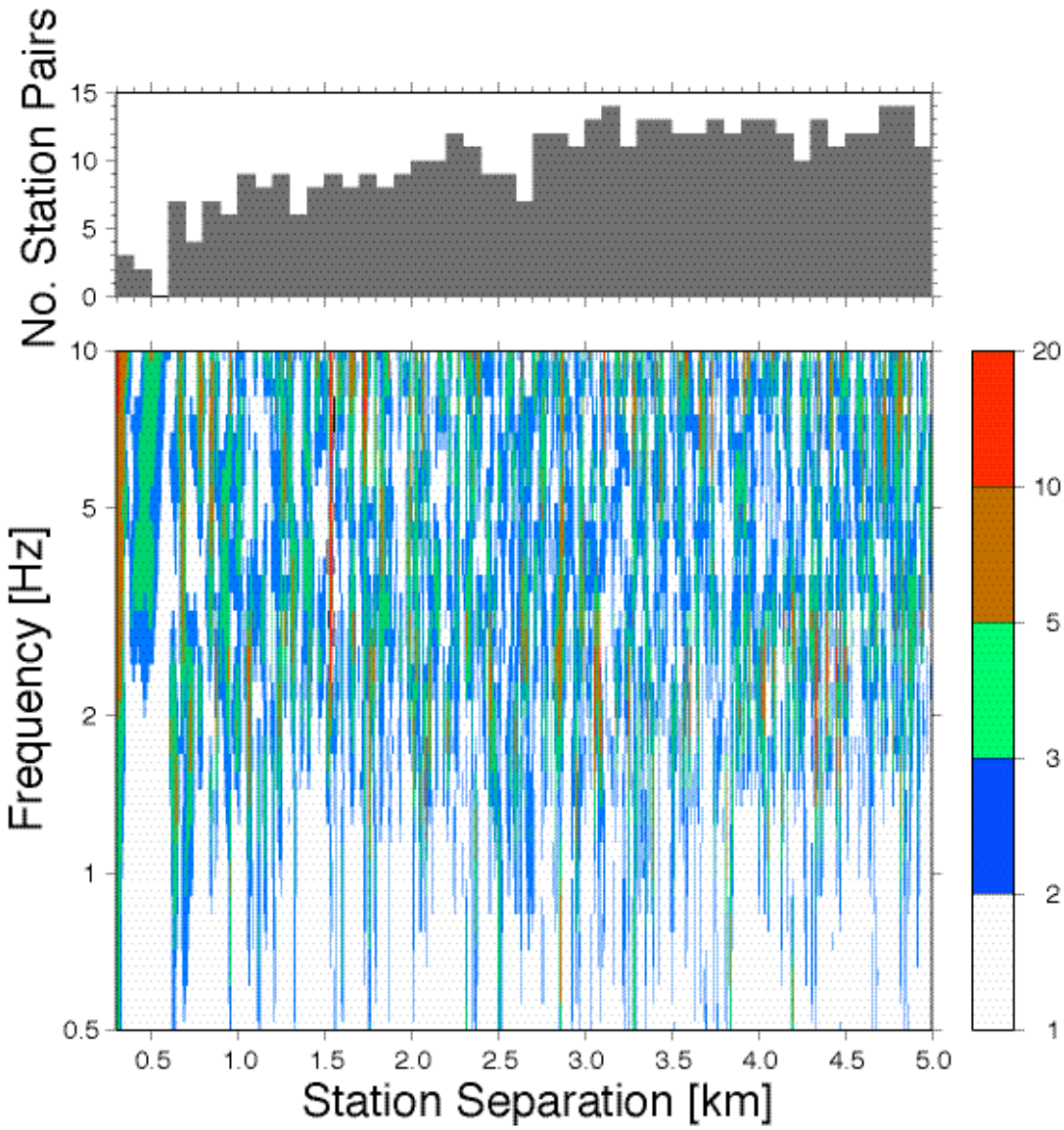

Figure 5: A contour plot of the site response coefficients $SRC(f)$ from 466 distinct station pairs with a separation distance between 119 m and 5 km. We smoothed over a distance of 5 m and over frequency interval of 0.25 Hz. Although there is spatial variability, the site response coefficient is generally less than 2.0 (separation distances up to 5 km). As expected, there is more variation in the site response coefficient for the higher frequencies. Histogram at the top indicates the number of station pairs within 100 m intervals. Although there a few station pairs with distances less than 300 m, there are several gaps in the station separation distance. To avoid contouring artifacts resulting from the gaps, such as that between 0.5-0.6 km, we consider station separations greater than 300 m.

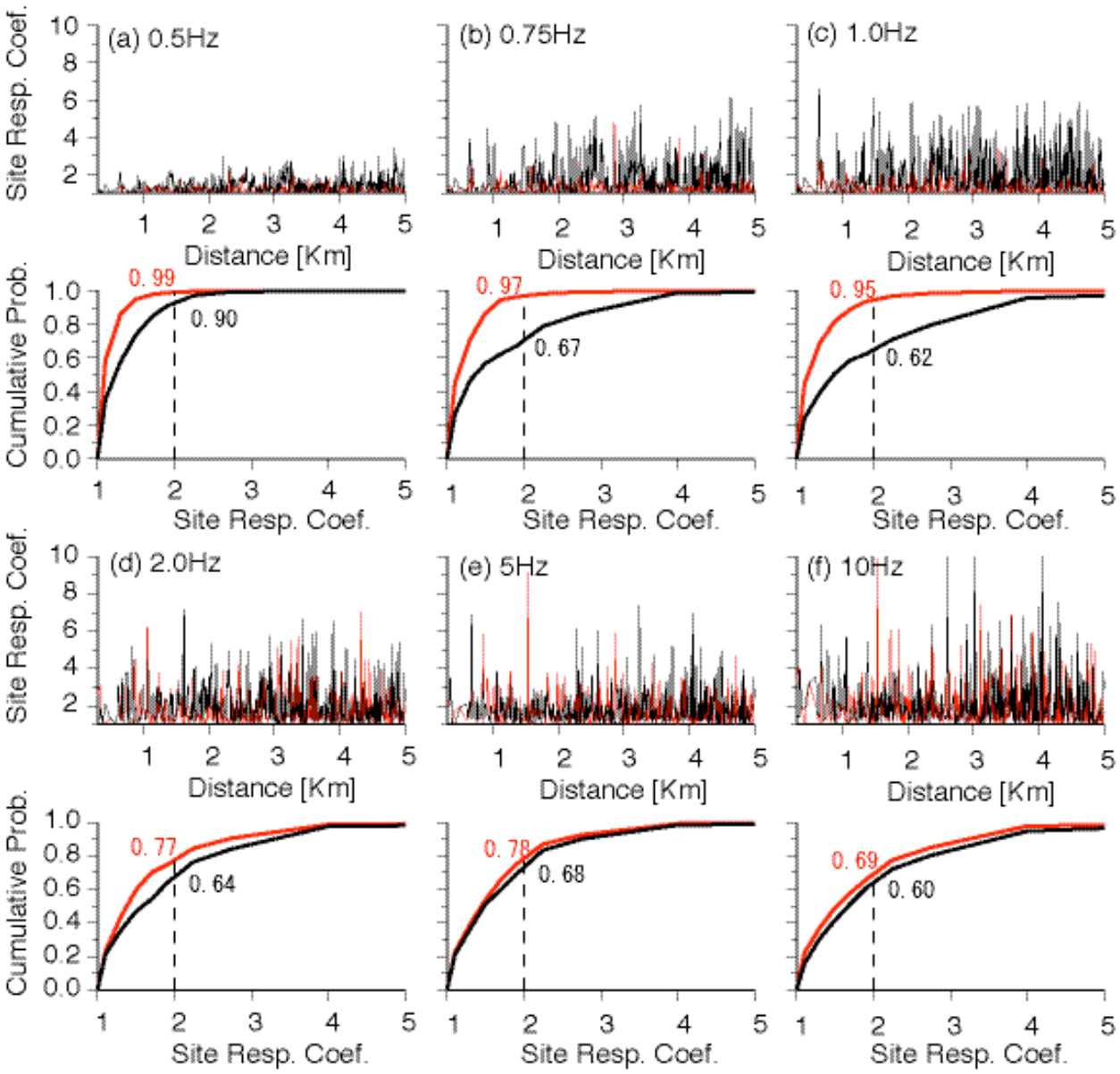

Figure 6: For 6 central frequencies we show the site response coefficients as a function of station separation (upper panel) and cumulative probability as function of site response coefficients (lower panel). Red lines correspond to pairs of stations with the most similar AVS30; black lines correspond to pairs of stations with the least similar AVS30. The value listed on each of the lower panels corresponds to the cumulative probability where the site response coefficient is equal to 2. The plots show that for frequencies up to 1.0 Hz, there is a 95% probability that an unknown site response will be within a factor of 2 of a known site response if the two sites, with similar AVS30, are within 5 km of each other. The site response will be within a factor of 3 for 90% of the station pairs with similar AVS30. For station pairs with the least similar AVS30, there is an 80% chance at all six frequencies that the site response will be within a factor of 3.